Functionalization of Zeolite ZSM-5 by Hydrosilylation and Acetone Coupling: Synthesis, MAS NMR, and Theory

Saifudin M. Abubakar, Jeffrey C. Lee, David M. Marcus, Justin O. Ehresmann, and James F. Haw*

Department of Chemistry, University of Southern California, University Park, Los Angeles, California 90089-1661

Received: March 22, 2006; In Final Form: June 6, 2006

We report a two-step postsynthetic functionalization reaction of zeolite HZSM-5 that proceeds with high selectivity at room temperature. In the first step the framework acid sites of the zeolite are reacted with phenylsilane to replace the acidic proton with a hydrosilyl ($-SiH_3$) group covalently linked to the framework. This group readily couples to acetone in a second step to form a framework-bound hydrosilyl isopropyl ether that is thermally stable at 473 K, but decomposes in the presence of moisture. We characterized these reactions using ^{29}Si, ^{1}H, and ^{13}C MAS NMR, as appropriate. Theoretical modeling using density functional theory and cluster models of the zeolite acid site confirmed that both steps were exothermic and provided theoretical chemical shift values in excellent agreement with experiment.

Introduction

Zeolites are widely used as sorbents, catalysts, and catalyst supports.[1−3] Postsynthetic modification of zeolites[4,5] is an attractive strategy for restricting the effective channel dimensions of the zeolite, reducing the number of framework acid sites, or introducing new chemical functionality. Recently we reported the functionalization of large-pore zeolite H-Beta (BEA topology) by reaction with trimethylphenylsilane as shown in Scheme 1.[6] This reaction, which was carried out in a plug flow reactor at 648 K, converted some of the acid sites to their trimethylsilyl derivatives.

As an extension of this work we report here the hydrosilylation of acid sites in the medium-pore zeolite HZSM-5 (MFI topology) by reaction with phenylsilane (Scheme 2). HZSM-5, one of the most commonly used zeolites, is characterized by two sets of intersecting channels, each defined by 10-member rings with channel diameters of 0.51−0.56 nm.[7,8] As we were aware that hydrosilanes couple with ketones under some conditions,[9,10] we extended our functionalization study to include the further step of coupling with acetone as in Scheme 3 to provide the hydrosilyl isopropyl ether derivative. Both reaction steps were carried out with vacuum line methods at moderate temperatures to facilitate addition of reactive or stable isotope chemicals and characterization of the products of each step with ^{29}Si, ^{13}C, and ^{1}H MAS NMR spectroscopy.

To firmly establish our NMR assignments of the products of Schemes 2 and 3 we used a cluster model of the acid site of zeolite HZSM-5 and density functional theory to model the energetics of the two reaction steps and to estimate values of the isotropic chemical shifts for comparison with experiment. These calculations showed that both reaction steps were exothermic, the second one especially so. Theoretical and experimental shifts were in excellent agreement with our proposed assignments for the experimental results.

We note that silylation of zeolites with either SiH_4 or Si_2H_6 followed by calcinations in air is commonly studied as a means to restrict channel size by the formation of amorphous silicious material.[11,12] Also, reaction with Si_2H_6 can sometimes result in well-characterized zeolite derivatives.[13] Finally, in the course of this study we became aware of a recent photoluminescence study in which the supercages of zeolite HY were reacted with phenylsilane, and the formation of hydrosilylated acid sites was confirmed by IR spectroscopy.[14]

We have not evaluated the reaction products of either Scheme 2 or Scheme 3 in practical applications as catalysts or catalyst

SCHEME 1

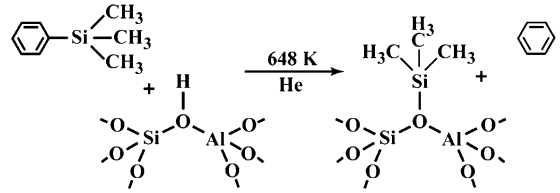

SCHEME 2

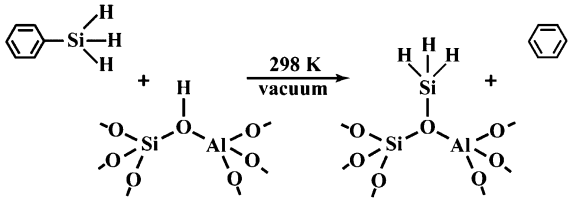

SCHEME 3

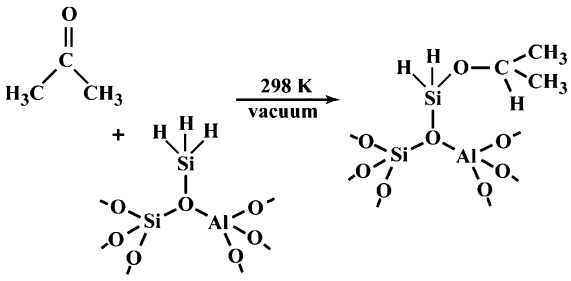

* To whom correspondence should be addressed. E-mail: jhaw@usc.edu.

10.1021/jp061791f CCC: $33.50
Published on Web 07/11/2006

supports; however, using high-temperature MAS NMR we established that the acetone coupling product is completely stable for 1 h at 473 K, except in the presence of moisture. Thus, we are encouraged that chemical transformations of the type reported here are at least potentially useful and related lines of investigation might find practical value.

Experimental Section

Computational Modeling. In common with some of our previous work we used a cluster model to approximate the acid site in zeolite HZSM-5.[15,16] Optimizations were performed with the B3LYP functional and the DZVP2 basis sets.[17] Chemical shifts were also calculated at B3LYP except with the tzplarge basis sets.[18,19] All computations were carried out with Gaussian 03.[20]

Materials and Reagents. Zeolite HZSM-5 (CBV 8014, $SiO_2/Al_2O_3 = 80$) was obtained from Zeolyst International. The zeolite was calcined at 873 K for 16 h prior to use to remove the remaining templating agent and pressed into 10−20 mesh pellets. Acetone-*2*-^{13}C (99 atom %) and phenylsilane (97%) were purchased from Aldrich while acetone-d_6 was purchased from Cambridge Isotope.

Zeolite Functionalization. All modification reactions were carried out with vacuum line methods and a shallow bed CAVERN apparatus[21] to hold the MAS rotor. Typically, 0.3 g of zeolite was loaded into the CAVERN, which was subsequently connected to a vacuum line. The zeolite was heated to a final temperature of 673 K with a heating rate of 0.7 deg/min and kept at the final temperature for 12 h under vacuum. Phenylsilane, typically 0.122 mmol, was then introduced to the catalyst at 298 K for 30 min. The silylated zeolite was then either sealed in the MAS rotor or further modified by reaction with acetone. In the latter case the silylated zeolite was evacuated at 353 K for 30 min to remove the benzene liberated in the first reaction step. Then at 298 K either acetone, acetone-*2*-^{13}C, or acetone-d_6 (typically 0.122 mmol) was adsorbed and allowed to react for 30 min before sealing the rotor for NMR studies.

In Situ MAS NMR Spectroscopy. A Chemagnetics CMX-360 NMR spectrometer operating at 71.5 MHz for ^{29}Si, 90.5 MHz for ^{13}C, 93.7 MHz for ^{27}Al, and 359.7 MHz for ^{1}H was used for all the MAS NMR spectroscopy. TMS (0 ppm), HMB (17.3 ppm), 1.0 M $Al(NO_3)_3$ (0 ppm), and TMS (0 ppm) were used as external chemical shift standards for ^{29}Si, ^{13}C, ^{27}Al, and ^{1}H, respectively. A Chemagnetics-style pencil probe spun 7.5 mm zirconia rotors at 5.5−6.0 kHz with active spin speed control (±3 Hz). All spectra shown were obtained at room temperature with Bloch decay, except where otherwise stated. ^{29}Si Bloch decay MAS NMR spectra were acquired with proton decoupling with use of 2000 scans, 90° flip angle, and 30 s pulse delays. Additionally ^{29}Si CP/MAS NMR spectra were acquired with 40 000 scans, 90° flip angle, 3.5 ms contact time, 2 s pulse delays, and proton decoupling. ^{13}C Bloch decay MAS NMR spectra were acquired with proton decoupling with use of 1000 scans, 90° flip angle, and 10 s pulse delays. ^{13}C CP/MAS NMR spectra were acquired with 2000 scans, 90° flip angle, 2 ms contact time, proton decoupling, and 1 s pulse delays. ^{27}Al Bloch decay MAS NMR spectra were acquired with 10 000 scans, 15° flip angle, and 3 s pulse delays. ^{1}H MAS NMR spectra were acquired with 32 scans, 90° flip angle, and 15 s pulse delays.

Results

Computational Modeling. Our computational results are presented in Figures 1 and 2 for the products of zeolite silylation and acetone coupling, respectively. These figures more precisely introduce the structures of the two reaction products and provide a guide to the eye in the interpretations of the NMR experimental results to follow. Our calculations modeling the reaction of an unmodified acid site with phenylsilane (as in Scheme 2) to form the structure in Figure 1 found a ΔE of −13 kcal/mol. The structure in Figure 1 has an elongated framework Al−O bond at the reaction site, 1.83 Å vs an average of 1.66 Å for the

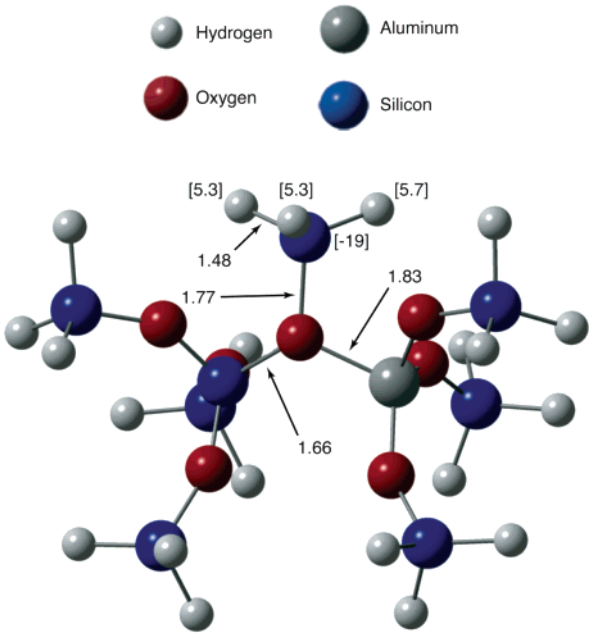

Figure 1. B3LYP/DZVP2 optimized structure for the framework-bound hydrosilyl species on a cluster model of the framework Brønsted acid site of zeolite HZSM-5. Selected bond distances (Å) and [isotropic chemical shifts] are indicated on the figure.

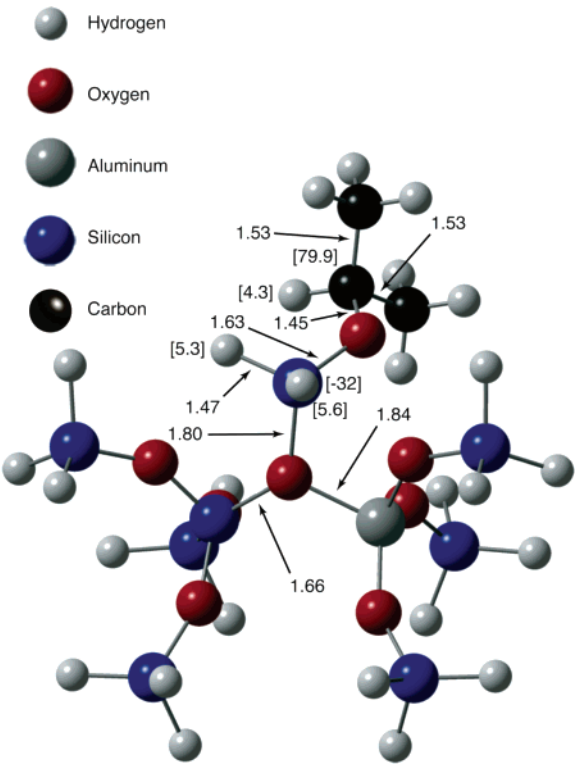

Figure 2. B3LYP/DZVP2 optimized structure of the framework-bound hydrosilyl isopropyl ether species on a cluster model of the framework Brønsted acid site of zeolite HZSM-5. Selected bond distances (Å) and [isotropic chemical shifts] are indicated on the figure.

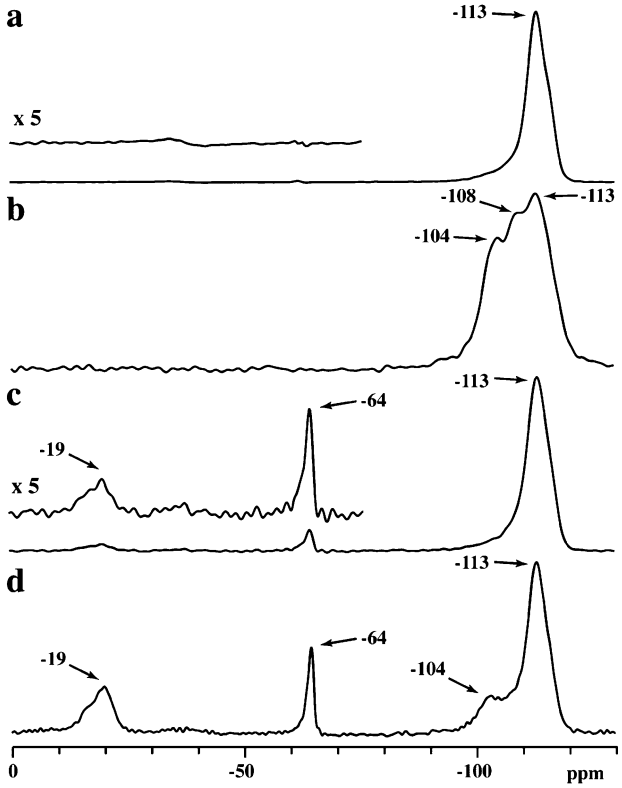

Figure 3. ^{29}Si MAS NMR spectra show a distinct change in the silicon framework of the zeolite following modification of HZSM-5 (Si/Al = 40) with phenylsilane. Standard HZSM-5 (Si/Al = 40) calcined at 823 K overnight: (a) Bloch decay and (b) cross-polarization. HZSM-5 (Si/Al = 40) after treatment with 1.1 equiv (with respect to Brønsted acid sites) of phenylsilane at 298 K: (c) Bloch decay and (d) cross-polarization. The peak at −19 ppm is assigned to framework-bound hydrosilyl groups ($OSiH_3$) while the peak at −64 ppm is characteristic of phenylsilane. Upon integration of the area under the curves (Bloch decay), the ratio of framework silicon to framework-bound hydrosilyl groups is approximately 40. The spinning speed for all experiments was 5.5 kHz. Bloch decay spectra (4000 scans) were acquired at 298 K with a 30 s pulse delay while the cross-polarization spectra (40 000 scans) were measured at 298 K with a 3.5 ms contact time and 2 s pulse delay.

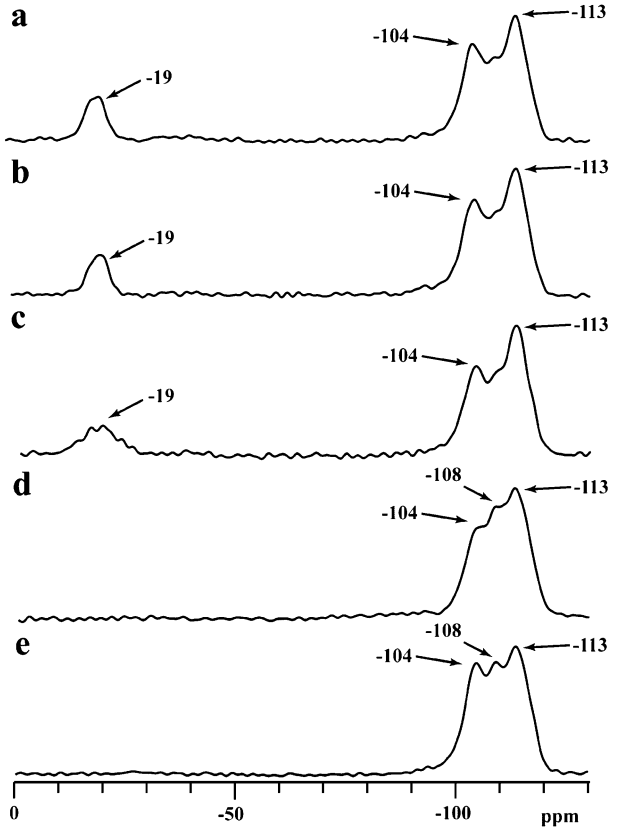

Figure 4. ^{29}Si CP MAS NMR spectra from CAVERN experiments of HZSM-5 (Si/Al = 40) treated with (a) 0.5 equiv of phenylsilane at 298 K (standard cross-polarization with decoupling), (b) 0.5 equiv of phenylsilane at 298 K (cross-polarization with interrupted decoupling $-\tau = 50\ \mu$s), (c) 0.5 equiv of phenylsilane at 298 K (cross-polarization with no decoupling), (d) 0.5 equiv of phenylsilane at 298 K followed by exposure to air (standard cross-polarization), and (e) 0.5 equiv of silane at 298 K (standard cross-polarization). The peak at −19 ppm (seen in spectra a−c in Figure 4), assigned to the framework-bound hydrosilyl group ($OSiH_3$), survives interrupted decoupling but broadens visibly when there is no decoupling. Upon exposure to air, the framework-bound hydrosilyl group ($OSiH_3$) hydrolyzes. In contrast, silane has no reaction with HZSM-5 under identical conditions. The signal at −104 ppm is due to surface silanols. The spinning speed for all experiments was 5.5 kHz. All spectra (40 000 scans) were acquired at 298 K with a 3.5 ms contact time and 2 s pulse delay.

remaining three Al−O bonds. This compares with 1.83 and 1.66 Å for the corresponding distances in the unmodified acid site cluster. Thus, the silylated site has the same structural distortion as the unmodified acid site. The $O-SiH_3$ distance is 1.77 Å, and the Si−H distance is 1.48 Å compared to 1.49 Å in phenylsilane at the same level of theory. Further reaction of the silylated zeolite to form the acetone adduct as shown in Figure 2 occurs with a theoretical ΔE of −160 kcal/mol. This compares with −30 kcal/mol for the analogous reaction of phenylsilane and one acetone at the same level of theory. The bond distances shown in Figure 2 are unremarkable. Selected isotropic chemical shifts for ^{29}Si, ^{13}C, and ^{1}H (B3LYP/tzplarge) are shown in Figures 1 and 2 as numbers in square brackets.

Hydrosilylation of HZSM-5 Zeolite. The ^{29}Si MAS NMR spectra in Figure 3 provide strong experimental evidence of the reaction step in Scheme 2. Spectra a and b in Figure 3 are spectra of the unmodified zeolite obtained with Bloch decay and cross polarization, respectively. The signal at −113 ppm, which dominates the more quantitative Bloch decay spectrum, is characteristic of the great majority of internal framework silicons remote from acid sites.[22,23] The cross-polarization (CP) spectrum emphasizes contributions from silicons close in space to protons; the signal at −108 ppm is due to silicons with an aluminum nearest neighbor, and it is a measure of unmodified framework acid sites. Our assignment of this signal is consistent with the values predicted by our DFT calculation in Figure 1.

The ^{29}Si spectra in Figure 3c,d were obtained after adsorption of a slight excess of phenylsilane at room temperature. The −108 ppm signal due to acid sites is largely absent from Figure 3d following phenylsilane adsorption, and it is replaced by a new signal at −19 ppm that we assign to the silylated product of the acid sites. Also present is a signal at −64 ppm, the exact value expected for excess or unreacted phenylsilane. It is likely that neither spectrum is fully quantitative as a result of long and variable ^{29}Si T_1 values as well as differences in cross-polarization dynamics between bound and mobile species. The signals at −104 ppm in the CP spectra (Figures 3b,d) are due to surface silanols.

Figure 4 reports ^{29}Si MAS spectra that further establish the assignment of the −19 ppm peak as well as its chemistry. The dipolar dephasing spectrum in Figure 4b is almost identical with the standard CP spectrum in Figure 4a, consistent with the assignment of $-SiH_3$, a functional group analogous (in NMR and dynamical properties) to $-CH_3$. Figure 4c shows that this signal is broadened by turning off the decoupler during spectral

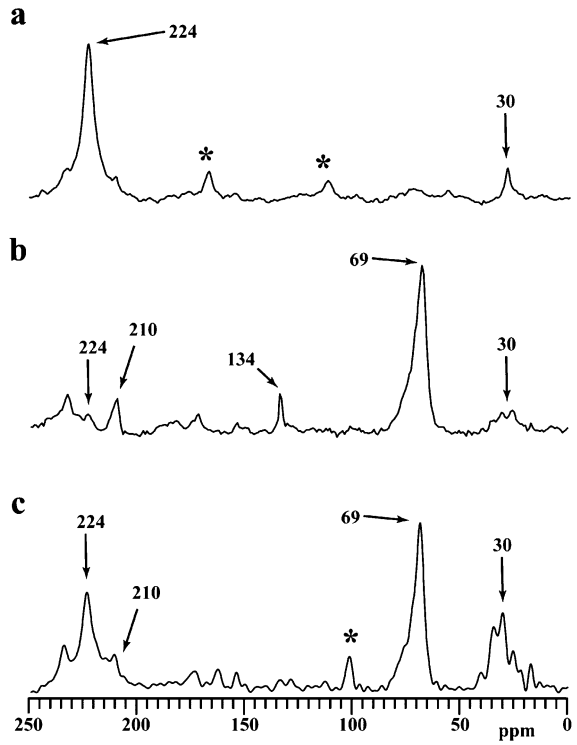

Figure 5. ^{13}C CP/MAS NMR spectra of (a) 1.0 equiv of acetone-*2*-$^{13}C_2$ absorbed on standard HZSM-5 (Si/Al = 40) at 298 K, (b) 1.0 equiv of acetone-*2*-$^{13}C_2$ absorbed on phenylsilane treated HZSM-5 (Si/Al = 40) at 298 K, and (c) 1.0 equiv of acetone-*2*-$^{13}C_2$ absorbed on phenylsilane treated HZSM-5 (Si/Al = 40) followed by heating at 473 K for 1 h. There are three main peaks at 69, 210, and 224 ppm following the acetone-*2*-$^{13}C_2$ treatment. The 210 and 224 ppm peaks are assigned to carbonyl carbon of the acetone and mesityl oxide interacting with the Brønsted acid sites. The peak at 69 ppm, assigned to the formation of isopropoxy carbon bound to the hydrosilyl group, increases in intensity with cross-polarization. Upon heating to 473 K, the majority of the isopropoxy groups survive. The spinning speed for all experiments was 5.5 kHz. Cross-polarization spectra (2000 scans) were acquired at 298 K with use of a 4 ms contact time and 2 s pulse delay.

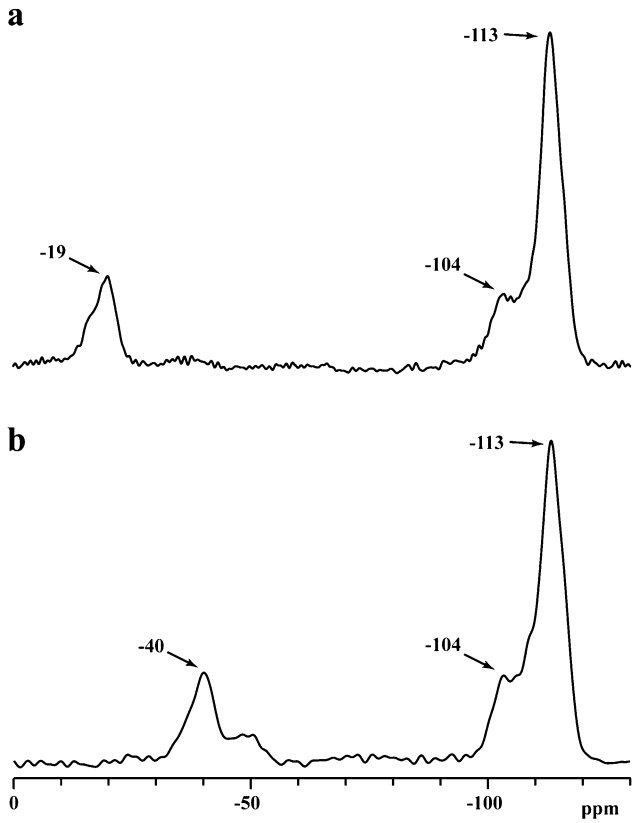

Figure 6. ^{29}Si CP MAS NMR spectra from CAVERN experiments of HZSM-5 (Si/Al = 40) treated with (a) 1.1 equiv of phenylsilane followed by evacuation at 393 K and (b) 1.1 equiv of phenylsilane, evacuated followed by 1.0 equiv of acetone-*2*-$^{13}C_2$ adsorption at 298 K. The peak at −19 ppm, assigned to the framework-bound silyl group ($OSiH_3$), shifted upfield to −40 ppm due to the presence of two oxygen atoms directly attached to it. The spinning speed for all experiments was 5.5 kHz. All spectra (40 000 scans) were acquired at 298 K with use of a 3.5 ms contact time and 2 s pulse delay.

acquisition, again consistent with the proposed assignment. The framework $-SiH_3$ group is not stable to exposure to atmosphere; as shown in Figure 4d the feature disappears entirely (presumably in the formation of amorphous silica) after air exposure at room temperature. Finally, Figure 4e is a ^{29}Si CP spectrum of a sample of HZSM-5 exposed to SiH_4 under conditions identical with those used to form the hydrosilyl derivative from phenylsilane. In this case, however, there is no reaction to form the framework $-SiH_3$ derivative.

High-temperature ^{29}Si MAS spectra (not shown) demonstrated that the framework-bound hydrosilyl groups were stable at temperatures of at least 473 K. On the other hand, calcination in air at 773 K regenerated the Brønsted acid sites. NMR spectra showed no evidence of the $-SiH_3$ groups after calcination, and a cursory examination of the catalytic activity for methanol to hydrocarbon conversion showed that the calcined material was not obviously different from the original zeolite. We also used ^{27}Al MAS NMR (not shown) to establish that no de-alumination of the framework occurred either by reaction with phenylsilane or subsequent calcination.

Coupling of Framework Hydrosilyl Groups to Acetone. Figure 5 presents ^{13}C CP/MAS NMR spectra that serve to introduce the coupling reaction of acetone-*2*-^{13}C with framework bound hydrosilyl groups. Figure 5a is the spectrum (for comparison) of acetone-*2*-^{13}C on standard (untreated) HZSM-5. The spectrum is dominated by the resonance at 224 ppm previously assigned to the hydrogen-bonded complex of acetone and an acid site. When acetone-*2*-^{13}C is adsorbed at room temperature onto zeolite treated with phenylsilane and then evacuated at 353 K (to remove benzene) the spectrum in Figure 5b was obtained. This shows, primarily, an intense signal at 69 ppm. Also seen are small signals at 210 and 134 ppm that can be assigned, based on previous work,[24] to mesityl oxide, the dimeric product of aldol coupling and dehydration of acetone. Figure 5c is a similar spectrum acquired at room temperature after heating the sample to 473 K for 1 h in the NMR probe. This spectrum shows that the 69 ppm peak has largely survived the heating step.

Further evidence for the coupling reaction between acetone and the framework-bound hydrosilyl groups is afforded by the ^{29}Si spectra in Figure 6. Figure 6a is before adsorption of acetone, while Figure 6b shows that after acetone adsorption the resonance formerly at −19 ppm is replaced with a new peak at −40 ppm. The ^{1}H MAS spectra in Figure 7 correspond to the analogous ^{29}Si spectra in the previous spectrum. Adsorption of acetone results in a modest change in the location of the hydrosilyl resonance, from 5.1 to 5.0 ppm, but a new and distinct resonance appears at 3.5 ppm. It is possible that some exchange of the deuterons on the acetone used in this experiment may have occurred prior to coupling. If so that suggests an explanation for the 2.6 ppm peak in Figure 7b.

Discussion

Chemical Shift Assignments: Agreement between Theory and Experiment. Our evidence for the two reaction steps

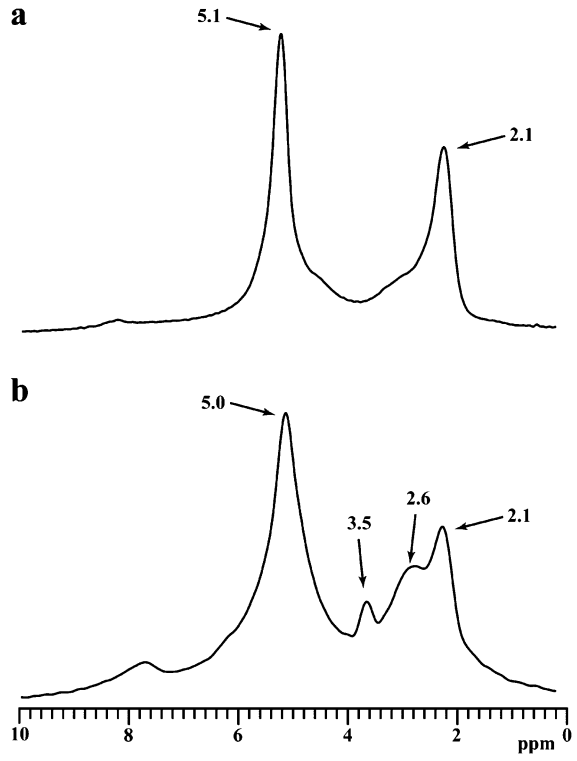

Figure 7. ^{1}H MAS NMR spectra from CAVERN experiments of HZSM-5 (Si/Al = 40) treated with (a) 1.1 equiv of phenylsilane followed by evacuation at 393 K and (b) 1.1 equiv of phenylsilane, evacuated followed by 1.0 equiv of acetone-d_6 adsorption at 298 K. The framework-bound silyl group transferred a hydride to the carbonyl carbon and an isopropoxy group is formed with a resulting chemical shift of 3.5 ppm. The peak at 2.6 ppm from the methyl group of mesityl oxide formed from acetone-d_6 on the Brønsted acid sites. The spinning speed for all experiments was 5.5 kHz. All spectra (32 scans) were measured at 298 K with a 10 s pulse delay.

proposed is almost entirely based on NMR chemical shifts. While all of the assignments are at least qualitatively reasonable we took advantage of computational predictions to attempt a more quantitative assignment. The calculated (B3LYP/tzplarge) isotropic chemical shifts in Figures 1 and 2 are generally in excellent agreement with experiment. The tzplarge basis set is well suited to ^{13}C and ^{29}Si shifts. GIAO-MP2 chemical shift calculations are clearly more accurate than GIAO-DFT calculations, but given the number of basis functions required (531 for Figure 1, and 645 for Figure 2) we were forced to use the less accurate, but still useful GIAO-B3LYP method.

The computed ^{29}Si isotropic chemical shift of the O−SiH_3 group (Figure 1) is −19 ppm, in perfect agreement with the experimental value. The O−SiH_2−O ^{29}Si shift is calculated to be −32 ppm versus −40 ppm experimental (Figure 6). The carbon derived from C_2 of acetone is predicted to be at 79.9 ppm, while it is only 69 ppm experimentally. To understand this discrepancy we optimized the structure of SiH_3−O−CH-$(CH_3)_2$ at B3LYP/DZVP2 and then computed the ^{13}C shift of C_2 at both B3LYP/tzplarge and MP2/tzplarge. These values were 77.4 and 66.3 ppm, respectively. Thus, all of the difference between the experimental result of 69 ppm in Figure 6 and the computational result of 79.9 ppm in Figure 2 can be rationalized by the deficiency of the B3LYP functional in this case. The profound change from the ^{13}C shift of acetone, 224 ppm in the zeolite complex to the value observed for the adduct in Figure 5, 69 ppm, can only be accounted for by an addition reaction converting this carbon from sp^2 to sp^3. The calculated ^{1}H shifts are uniformly in good agreement with experiment. The value for O−SiH_3 (Figure 1) of 5.4 ppm compares with an experimental value of 5.1 ppm (Figure 7), while the corresponding values for O−SiH_2−O are 5.5 (Figure 2) and 5.0 ppm (Figure 7). The O−CH hydrogen on the coupling product is predicted to be at 4.3 ppm and is observed at 3.5 ppm (Figure 7). The predicted ^{1}H shifts for the methyl groups of the adduct (∼1.5 ppm) probably account for the signal at 2.6 ppm in Figure 7b. Acetone-d_6 would readily undergo H/D exchange catalyzed by any remaining acid sites, so some signal due to methyl groups on the adduct would be unremarkable.

In summary, the agreement between theoretical and experimental chemical shifts is very satisfying and we have consider our theoretical modeling to provide very strong evidence in support of our proposed assignments of the framework silyl species and its acetone adduct.

Functionalization Chemistry. The use of phenyl as a leaving group permits the silylation reaction to occur at room temperature with phenylsilane while no reaction was observed under identical conditions with SiH_4. The Si−H bond strength is quite low as compared to Si−O, and hence the reaction with acetone was very favorable thermochemically. Similar reasoning would suggest that the framework-bound −SiH_3 group might be useful for a wide range of coupling reactions with other reagents. While we are encouraged by the ease with which we realized a two-step postsynthetic functionalization reaction linking an organic unit onto the framework of a zeolite, it must be emphasized that we have not yet sought to realize any practical catalysts, catalyst supports, or sorbents using this or similar chemistry.

Acknowledgment. This work was supported by the U.S. Department of Energy (DOE) Office of Basic Energy Sciences (BES) (Grant No. DE-FG03-99ER14956).

References and Notes

(1) Bailey, S. E.; Olin, T. J.; Bricka, R. M.; Adrian, D. D. *Water Res.* **1999**, *33*, 2469.
(2) Wight, A. P.; Davis, M. E. *Chem. Rev.* **2002**, *102*, 3589.
(3) Sachtler, W. M. H.; Zhang, Z. C. *Advances in Catalysis*; Elsevier Science: Amsterdam, The Netherlands, 1993; Vol. 39.
(4) Niwa M.; Kato S.; Hattori, T.; Murakami Y. *J. Chem. Soc., Faraday Trans. 2* **1984**, *80*, 3135.
(5) Impens, N. R. E. N.; van der Voort, P.; Vansant, E. F. *Microporous Mesoporous Mater.* **1999**, *28*, 217.
(6) Song, W.; Marcus, D. M.; Abubakar, S. M.; Jani, E.; Haw, J. F. *J. Am. Chem. Soc.* **2003**, *125*, 13964.
(7) Kokotailo, G. T.; Lawton, S. L.; Olson, D. H.; Meier, W. M. *Nature* **1978**, *272*, 437.
(8) Olson, D. H.; Kokotailo, G. T.; Lawton, S. L.; Meier, W. M. *J. Phys. Chem.* **1981**, *85*, 2238.
(9) Eaborn, C.; Bott, R. W. *Organometallic Conpounds of the Group IV Elements*; Marcel Dekker: New York, 1968; Vol. 1.
(10) Brook M. A. *Silicon in Organic, Organometallic, and Polymer Chemistry*; Wiley: New York, 2000.
(11) Mees, F. D. P.; Voort, P. V. D.; Cool, P.; Martens, L. R. M.; Janssen, M. J. G.; Verberckmoes, A. A.; Kennedy, G. J.; Hall, R. B.; Wang, K.; Vansant, E. F. *J. Phys. Chem. B.* **2003**, *107*, 3161.
(12) Yan, Y.; Vansant, E. F. *J. Phys. Chem.* **1990**, *94*, 2582.
(13) Yan, Y.; Vansant, E. F. *J. Phys. Chem.* **1995**, *99*, 14089.
(14) Tanaka, K.; Choo, C.-K.; Komatsu, Y.; Hamaguchi, K.; Yamaki, M.; Itoh, T.; Nishigaya, T.; Nakata, R.; Morimoto, K. *J. Phys. Chem. B* **2004**, *108*, 2501.
(15) Haw, J. F.; Nicholas, J. B.; Xu, T.; Beck, L. W.; Ferguson, D. B. *Acc. Chem. Res.* **1996**, *29*, 259−267.
(16) Ehresmann, J. O.; Wang, W.; Herreros, B.; Luigi, D. P.; Venkatraman, T. N.; Song, W.; Nicholas, J. B.; Haw, J. F. *J. Am. Chem. Soc.* **2002**, *124*, 10868−10874.
(17) Becke, A. D. *J. Chem. Phys.* **1993**, *98*, 5648.
(18) Godbout, N.; Salahub, D. R.; Andzelm, J.; Wimmer, E. *Can. J. Chem.* **1992**, *70*, 560.
(19) Schafer, A.; Huber, C.; Ahlrichs, R. *J. Chem. Phys.* **1994**, *100*, 5829.
(20) Frisch, M. J.; Trucks, G. W.; Schlegel, H. B.; Scuseria, G. E.; Robb, M. A.; Cheeseman, J. R.; Montgomery, J. A., Jr.; Vreven, T.; Kudin, K.

N.; Burant, J. C.; Millam, J. M.; Iyengar, S. S.; Tomasi, J.; Barone, V.; Mennucci, B.; Cossi, M.; Scalmani, G.; Rega, N.; Petersson, G. A.; Nakatsuji, H.; Hada, M.; Ehara, M.; Toyota, K.; Fukuda, R.; Hasegawa, J.; Ishida, M.; Nakajima, T.; Honda, Y.; Kitao, O.; Nakai, H.; Klene, M.; Li, X.; Knox, J. E.; Hratchian, H. P.; Cross, J. B.; Bakken, V.; Adamo, C.; Jaramillo, J.; Gomperts, R.; Stratmann, R. E.; Yazyev, O.; Austin, A. J.; Cammi, R.; Pomelli, C.; Ochterski, J. W.; Ayala, P. Y.; Morokuma, K.; Voth, G. A.; Salvador, P.; Dannenberg, J. J.; Zakrzewski, V. G.; Dapprich, S.; Daniels, A. D.; Strain, M. C.; Farkas, O.; Malick, D. K.; Rabuck, A. D.; Raghavachari, K.; Foresman, J. B.; Ortiz, J. V.; Cui, Q.; Baboul, A. G.; Clifford, S.; Cioslowski, J.; Stefanov, B. B.; Liu, G.; Liashenko, A.; Piskorz, P.; Komaromi, I.; Martin, R. L.; Fox, D. J.; Keith, T.; Al-Laham, M. A.; Peng, C. Y.; Nanayakkara, A.; Challacombe, M.; Gill, P. M. W.; Johnson, B.; Chen, W.; Wong, M. W.; Gonzalez, C.; Pople, J. A. *Gaussian 03*, Revision C.02; Gaussian, Inc.: Wallingford CT, 2004.

(21) Xu, T.; Haw, J. F. *Top. Catal.* **1997**, *4*, 109.

(22) Engelhardt, G.; Michel, D. *High-Resolution Solid State NMR of Silicates and Zeolites*; John Wiley and Sons: New York, 1987.

(23) Fyfe, C. A.; Feng, Y.; Grondey, G.; Kokotailo, G. T.; Gies, H. *Chem. Rev.* **1991**, *91*, 1525.

(24) Xu, T.; Munson, E. J.; Haw, J. F. *J. Am. Chem. Soc.* **1994**, *116*, 1962.